Numerical Study On Multi Layered Target Material Subjected To Impact Loading

Abstract

In this study, the glass/epoxy composite laminate is layered with polyure-thane foam/ polyurethane sheet and silicon carbide to analyse their re-sponse during high mass and low velocity impact. The silicon carbide is layered in two forms, one is as plate and the other is as inserts. The target materials are prepared in various combinations and the bonding of layers is done by using epoxy. Effectiveness of silicon carbide inserts and plates are compared in terms of their energy absorbing capacities. The numerical simulation is also carried for the target material with the same experi-mental conditions. The experimental results are compared with the numer-ical results for validation and a reasonably good agreement is found. Fur-ther, the validated numerical model is extended to understand the ballistic performance of the target material. It is observed that the introduction of silicon carbide as front layer improves both the structural and ballistic per-formance. Also, the damage in case of samples with silicon carbide inserts is localized as opposed to that of silicon carbide plate.

Keywords

Impactor; SiC inserts; Gas Gun; Ballistic limit; GFRP

Vishwas Chandra Khan[a*]
Akshaj Kumar Veldanda[a]
G Balaganesan[b]
M S Sivakumar[b]

[a]Indian Institute of Technology Bhubaneswar, Bhubaneswar, 752050, India, E-mails: vk13@iitbbs.ac.in; akv12@iitbbs.ac.in

[b]Indian Institute of Technology Madras, Chennai, 600036, India. E-mails: gbganesh@iitm.ac.in; mssiva@iitm.ac.in

*Corresponding author

1 INTRODUCTION

The necessity of human protection against the increasing threat levels of impact has led to the development of vehicle, aircraft and body armors. These armors must be designed to enhance mobility with high strength to weight ratio and, impact resistance. The concept of light weight armors led to the development of non-metallic materials for ballistic protection during projectile impact. Composite laminates were developed to meet these characteristics. Several impact studies were conducted to find the ballistic limit and energy absorbing capacity of composite laminates. It is necessary to understand and quantify the energy absorbed by each of the failure mech-anisms to design composite structures for ballistic impact applications. Wilkins (1978), Bhatnagar (2006), Velmurugan and Balaganesan (2013), Karandikar (2009) and Balaganesan et al. (2014) studied the energy ab-sorbing mechanisms in fiber reinforced polymer matrix composites and it was identified as elastic deformation of fibers, tensile failure of primary fibers, delamination and matrix crack. A basic armor system consists of front fac-ing hard ceramic tiles and a composite backing material. Naik et al. (2012) explained the damage sequence during impact phenomenon on ceramic-composite armor. They developed an energy-based dynamic analytical model for ballistic impact and found that the residual velocity values are having good agreement with their experimental results. Krishnan et al. (2010) performed numerical analysis of ceramic composite armour using LS-DYNA. They used Johnson Holmquist model for ceramic and user defined material model was developed to characterize the ductile backing made of highly elastic ultra-high molecular weight polyethylene (UHMWPE). They have found good agreement between experimental and numerical data. Feli and Asgari (2011) presented a FE simulation of ceramic/composite armor impacted by tungsten projectile. Johnson-Cook and Johnson-Holmquist failure criteria were used for projectile and ceramic respectively. They observed that a conoid shape fragment broke down from ceramic tile and its semi-angle decreased upon increasing the initial velocity. Inai et al. (2003) studied the energy absorbing capacity of carbon fibre braided composite tubes and they found that it has capability to absorb large amount of energy as a function of the fiber orientation angle. Recently, researchers have started studying the post impact performance of repaired glass fibre/epoxy composite laminates. Balaganesan and Chandra Khan (2016) conducted medium velocity impact on repaired glass/epoxy composite laminates and found that the experimental

results were in good agreement with the numerical results. They concluded that repaired laminates absorbed 80% of the energy absorbed by the undamaged specimen during impact loading.

Hybrid structures are proposed recently for impact applications with energy absorbing polymers and foams. In ballistic applications, hybrid sandwich structures made from such core materials are preferred, since it not only reduces the overall weight of the composite but also enhances the stiffness to weight ratio and possess high energy absorbing capability during impact. Qiao et al. (2008) concluded that composite laminates and foam core sandwich structures has added advantages over the traditional materials like steel, aluminum and other metals. Velmurugan et al. (2006) studied the impact response of composite sandwich panels made of glass/epoxy/ polyurethane foam subjected to projectile velocity ranging from 30 m/s to 100 m/s. They proposed a mathematical model to predict energy absorption and ballistic limit of the panels which were successfully validated with that of experimental results. Akshaj et al. (2017) conducted low velocity impact experiments to study the dent resistance of sandwich specimen made of metal laminates skins and thermoplastics/polyurethane foam core. They found that low-density polyethylene foam was the best choice of core materials considered. Ghalami-Choobar and Sadighi (2014) used LS-DYNA to investigate the high velocity impact on sandwiched polyurethane (PU) core with fiber metal laminates skins and they observed that the delamination and de-bonding on the back skin is more as compared to front. Abdel-Nasser et al. (2016) presented numerical simulation of low and high velocity impact using commercially available package ABAQUS to determine the ballistic performance of the laminated composites by changing the lay-up sequence. Long et al. (2015) studied the delamination behavior of composite laminates under low-velocity impact by developing a damage model based on cohesive contact method and they found a good agreement with the experiments. Yazdani Nezhad et al. (2015), Sekine et al. (1998), Ghosh and Sinha (2005), Shim et al. (2000), Wang et al. (2013) and Zhang et al. (2014) conducted low velocity impact experiments as well as simulations on composite laminates and sandwiched panels to analyze their energy absorbing capacity and reported that sandwiched panel has higher energy absorbing capacity than standalone composite/ceramic/metal laminates.

Though, significant research is conducted on high velocity impact of armor materials to analyze their ballistic performance, very limited literature is available for the understanding of the structural performance of armor materials. Therefore, this study presents, low velocity - high mass impact behavior of armor materials. It is proposed to design the armor plate considering both protective and structural applications for vehicle, aircraft and body. This study also includes the choice of core material to improve the performance of armor by discussing the energy absorbing capacity of polyurethane foam (PUF) and polyurethane sheet (PUS). Effectiveness of Silicon Carbide (SiC) inserts and plates was also compared in terms of the energy absorbing capacities of the laminates. The drop weight experimental results were compared with the numerical results for validation and a reasonably good agreement was found. Previously, the authors of this paper conducted the experiments to validate an analytical model. The experimental data in our earlier study, Balaganesan et al. (2017) was used to validate the numerical model in this study. Further, the validated numerical model was extended to understand the high velocity impact behaviour of armour material configured laminates. It was observed that the introduction of SiC as front layer improves both the structural and ballistic performance. Also, the damage in case of samples with SiC inserts was localized as opposed to that of SiC plate.

2 EXPERIMENTS

2.1 Specimen fabrication

Glass fiber reinforced polymer (GFRP) laminates were made of three layers' thick glass fiber woven roving mat (WRM) of 610 gsm and commercially available epoxy (Araldite LY556, Hardener HY951) using hand layup technique. GFRP laminates were cut into 150mm by 150mm using circular saw cutter. 6mm thick SiC was cut into the size of 100mm by100mm and 25mm by 25mm inserts. Dummy aluminium inserts of same dimension as that of SiC inserts were used at places where there is no impact. However, 10mm thick SiC was cut into plate of size 100mm by 100mm. Figures 1(a) and 1(b) represent the schematic of specimen having SiC plate and inserts respectively. 10mm thick Polyurethane foam (PUF) of density 450 kg/m³ and 5mm thick polyurethane sheet (PUS) were cut to 150mm by 150mm respectively. All these laminates were bonded in various configurations using epoxy. Figure 2 represents the arrangements of specimen made of PUF, PUS and GFRP layers.
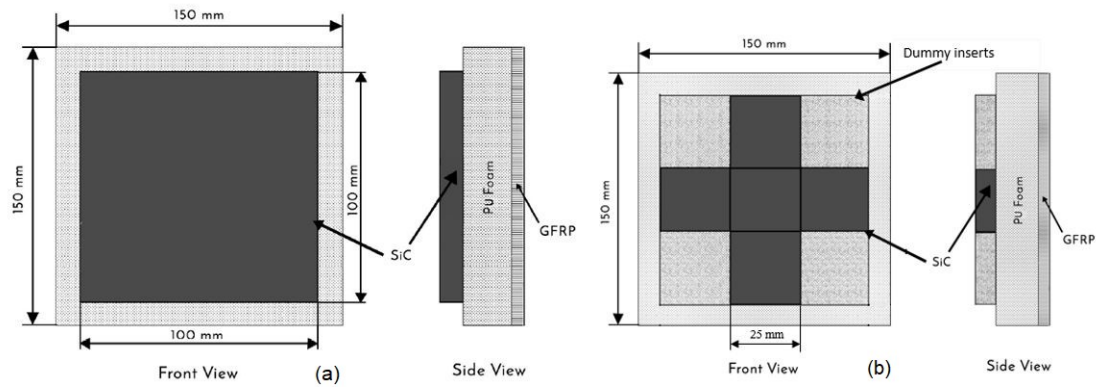
Figure 1: *(a) Schematic representation of specimen having front 6mm and 10mm sic plate, (b) Schematic representation of specimen having 6mm sic inserts*
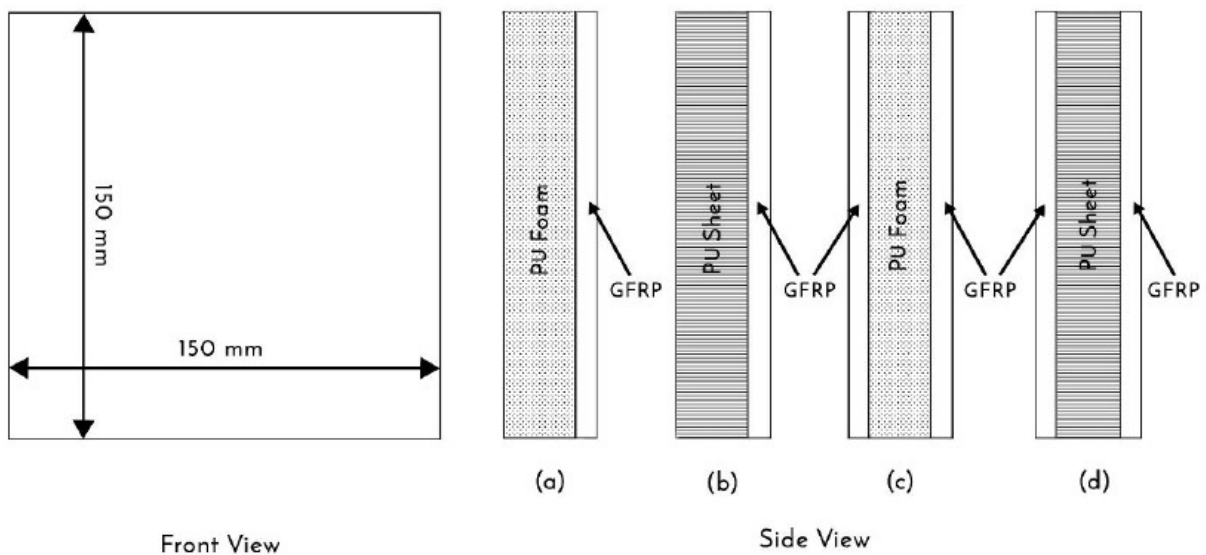

Figure 2: *Schematic representation of specimen having PUF, PUS and FRP layers*

2.2 Impact tests

Drop weight impact testing machine as shown in Figure 3 was used to conduct low velocity impact tests on specimens. Vertical guide rails ensure the point of impact in target plate when the impactor mass is released. A dynamic load cell was used to capture the impact force which was mounted to the cylindrical mild steel impactor of 16mm diameter. A rebound arrestor was used to avoid multi hits on the specimen by the impactor. For this study, impactor of mass 16 kg was dropped from a height of 0.5m, 1m and 1.5m. High speed camera was used to capture the impact and to measure the velocity of the impactor before and after the impact.
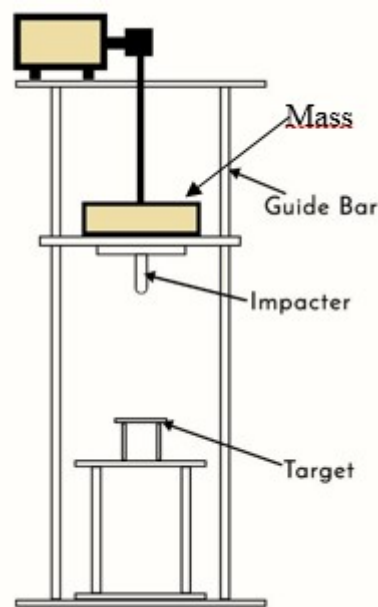
Figure 3: *Drop weight impact testing machine*

3 RESULTS

3. Material modelling and numerical simulation

Numerical simulation is carried using AUTODYN which is suitable program to simulate events such as impact, penetration, explosions and blast (Century Dynamics, 2013). The laminate is modeled as 100mm by100mm andthe edges are clamped rigidly. Many advanced material models are present in AUTODYN which can very closely characterize how the material will behave under impact loading.

The modeling is done using Solidworks and then the laminate is imported to ANSYS Explicit Dynamics where it is meshed using Lagrange approach. The final meshed model for low velocity and high velocity impact test is shown in Figures 4(a) and (b). Each element thickness is 2mm and bonding contact is assumed between the elements which depends on strength of the adhesive. The mesh is fine near the area of impact to capture the interaction between the target and projectile. The remaining area of target is done with coarse mesh to decrease the computational time. In the present analysis, SOLID185 element was used for the three-dimensional modelling of the laminates. The element is characterized by eight nodes and the orthotropic material properties having three degrees of freedom at each node and translations in the nodal x, y, and z directions. The element also has plasticity, stress stiffening, large deflection, and large strain capabilities which make it suitable for use in Explicit Dynamics problems. Finally, AUTODYN solver is used to simulate the target. As single point integration method is used that the elements have only one integration point at its centre, therefore, they are sensitive to the hourglassing problem. These zero energy modes produce rigid body motion and the mesh starts self-straining and destroying the solution. To prevent this phenomenon, hourglass coefficient had to be increased to 0.15, the minimum value which prevents the generation of spurious modes.
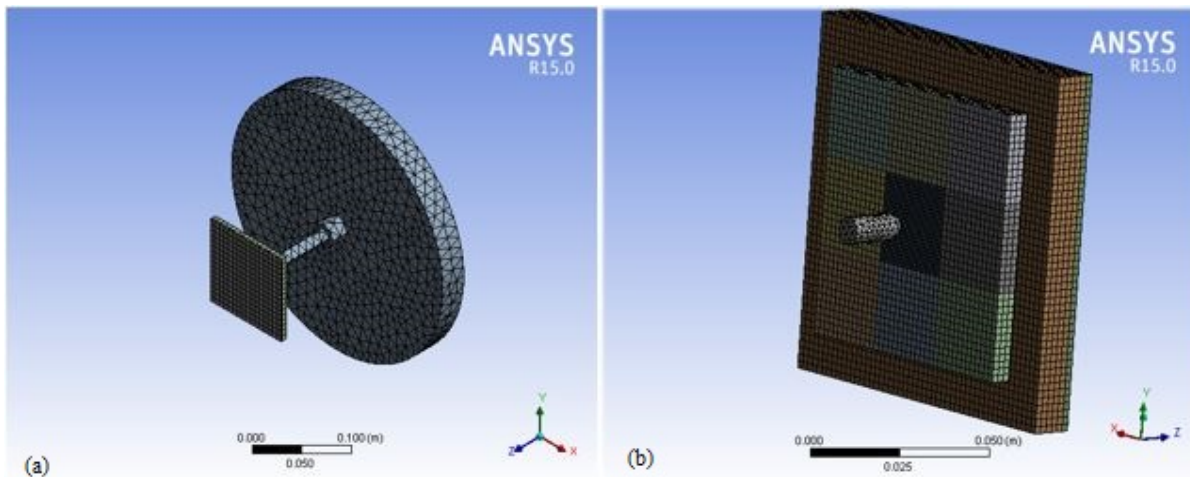
Figure 4: *(a) Numerical model of laminates for low velocity impact test, (b) numerical model of laminates for high velocity impact test*

3.1 Damage mechanism of ceramic

When the impactor impacts upon the ceramic plate the compressive shock waves are generated which propagate throughout the plate (Kauffmann et al., 2003). Once it reaches to the rear face it reflects and becomes a tensile wave which breaks the ceramic if the magnitude of the tensile wave is more than the tensile strength of ceramic (Krishnan et al., 2010). Also, there will be formation of micro cracks which will turn into macro cracks as the time progresses. During this period, more micro cracks will form and finally the ceramic will be broken in granules and powder (Wang et al., 2013). In case of a ductile or flexible backing, the effect of ceramic layer will be enhanced because part of compressive waves will be transmitted to the ductile or flexible backing.

3.1.1 The Johnson-Holmquist models for ceramic

The Johnson–Holmquist (JH) models are constitutive models suitable for predicting the behavior of brittle materials like ceramics subjected to extreme loading. There are two common models namely JH-1 (Johnson and Holmquist, 1990) and JH-2 (Johnson and Holmquist, 1994) used for numerical analysis of ceramics. In the present study, JH-1 model present in AUTODYN is used. In JH-1 model, the material stress is described in the form of linear segmented curve of equivalent stress versus pressure (Holmquist and Johnson, 2002). It is illustrated in Fig. 5. At a given pressure, if strain rate increases, then equivalent stress also increases, this makes the material stronger. But when there is material damage under a given pressure, it will reduce the equivalent stress and hence make the material weaker. The ratio of the total accumulated increment of plastic strain and the equivalent failure strain is termed as damage factor. The material will undergo failure, if negative pressure reaches the tensile limit T or damage factor D is equal to 1.0. Once the material is failed, it cannot withstand any tensile loading but can take some limited amount of compressive loading (Quan et al., 2006). The material data for ceramic is directly taken from the AUTODYN library.
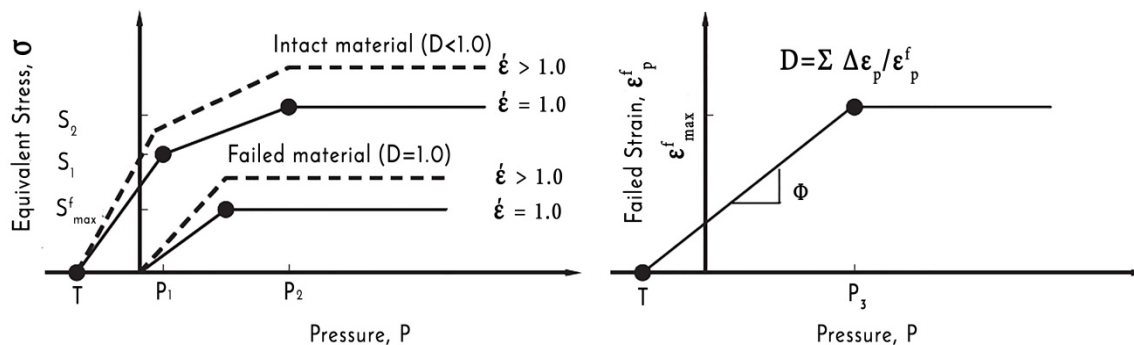

Figure 5: *Schematic explanation of JH-1 model (Holmquist and Johnson, 2002)*

3.2 The hyper-elastic model for Polyurethane polymer

There are various hyper-elastic models like Ogden model, the Van der Waals model, polynomial model etc. available to model the highly non-linear behavior of PU foam. In this paper, Ogden model (Ogden, 1972) is used and the material parameters are taken from the past work (Ferreño et al., 2010). They have also used closed cell PU foam of high density.

$$U = \sum_{i=1}^{N} \frac{2\mu_i}{\alpha_i^2}\left(\lambda_1^{\alpha_i} + \lambda_2^{\alpha_i} + \lambda_3^{\alpha_i} - 3\right) + \sum_{i=1}^{N} \frac{1}{D_i}\left(J^{e1} - 1\right)^{2i} \qquad (1)$$

N, μ_i, α_i and D_i are material parameters and N must be chosen a priori by the user.

Polyurethane sheet is modelled using linear equation of state, elastic strength model and principal stress failure criteria. The properties are directly taken from the AUTODYN library.

3.3 Composite Modeling

To understand ballistic impact of composite laminates, different failure mechanisms are to be analyzed. The energy absorbing mechanisms are moving cone formation on the back face of the target, elastic deformation and tensile failure of fibers, delamination and matrix crack (Morye et al., 2000). The orthotropic equation of state along with elastic strength model and material stress damage model is used to model the glass epoxy laminate. Delamination is assumed to result from excessive through-thickness tensile stresses or strains and/or from excessive shear stresses or strains in the matrix material. In the incremental constitutive relation below the stress $\Delta\sigma_{11}$ normal to the laminate and the corresponding orthotropic stiffness coefficients Cijare instantaneously set to zero, whenever the failure is initiated in either of those two modes, j=1 in equation (2):

$$\Delta\sigma_{jj} = 0 \ and \ C_{ij} = C_{ji} = 0 \ for \ i = 1, \ 3 \qquad (2)$$

$$
\begin{bmatrix}
\Delta\sigma_{11} \\
\Delta\sigma_{22} \\
\Delta\sigma_{33} \\
\Delta\sigma_{23} \\
\Delta\sigma_{31} \\
\Delta\sigma_{12}
\end{bmatrix}
=
\begin{bmatrix}
c_{11} & c_{12} & c_{13} & 0 & 0 & 0 \\
c_{12} & c_{22} & c_{22} & 0 & 0 & 0 \\
c_{13} & c_{23} & c_{23} & 0 & 0 & 0 \\
0 & 0 & 0 & \alpha C_{44} & 0 & 0 \\
0 & 0 & 0 & 0 & \alpha C_{55} & 0 \\
0 & 0 & 0 & 0 & 0 & \alpha C_{66}
\end{bmatrix}
\begin{bmatrix}
\Delta\epsilon_{11} \\
\Delta\epsilon_{22} \\
\Delta\epsilon_{33} \\
\Delta\epsilon_{23} \\
\Delta\epsilon_{31} \\
\Delta\epsilon_{12}
\end{bmatrix}
\qquad (3)
$$

Delamination will also occur with a reduction in shear stiffness αand a nominal value of 20% is used for α in the numerical simulations done in this paper. For impactor, the material, Steel 4340 is used which follows shock equation of state and Johnson Cook strength model.

3.5 Material properties

The properties of GFRP laminates are enlisted in the table 1 (Balaganesan and Chandra Khan, 2016). Glass fibres and resin are not separately modelled and the main phenomena of relevance are accounted for in an orthotropic model. Moreover, the bonding interaction between different layers is done using the normal stress limit and shear stress limit as input to the model. These values are assumed to be comparable to the properties of epoxy.

Table 1: *Material properties of the glass/epoxy laminate*

Property	Values	Property	Values
Equation of state	Orthotropic	G_{23}	3.49GPa
Reference density	1.87 g/cm³	G_{31}	3.22GPa
E_{11}	18.31GPa	σ_{11}	207.20MPa0
E_{22}	18.31GPa	σ_{22}	207.20MPa
E_{33}	3GPa	σ_{33}	61.23MPa
v_{12}	0.26	τ_{12}	50MPa
v_{23}	0.35	τ_{23}	40MPa
v_{31}	0.09	τ_{31}	30MPa
G_{12}	3.49GPa		

4. RESULTS AND DISCUSSION

4.1 Energy absorption in low velocity impact

The target specimens of various combinations of GFRP/ PUF/PUS are subjected to low velocity impact at incident energies of 80J, 160J and 240J. The experimental results are shown in Fig. 6. When the impactor of mass 16kg is dropped from a height of 0.5m, GFRP laminate absorb 17.73J of energy. Under the same impact conditions, the impactor penetrated through PUF+GFRP specimen which absorbed 48.58J of energy but failed to penetrate through PUS+GFRP laminate which absorbed 64.34J of energy. The later specimen initially absorbs complete 80J of energy and due to the elastic property of PUS, the specimen releases elastic energy to the impactor allowing it to rebound. While, in case of GFRP+PUS+GFRP, the impactor perforates and got struck in the specimen due to friction between impactor and top facing GFRP. In this case, the target material absorbs 67.49J of energy. In all other cases, the impactor is found to penetrate the target material. It is observed that specimen having PUS absorb more energy than the specimen having similar configuration but PUS replaced with PUF. PUS+GFRP absorbs 32%, 1.2% and 18% of energy more than PUF+GFRP at 80J, 160J and 240J of impactor incident energy respectively. Similarly, GFRP+PUS+GFRP absorbs 29%, 10% and 182% more than the energy absorbed by GFRP+PUF+GFRP at 80J, 160J and 240Jof impactor incident energy respectively.

Multi layered target material absorbs energy in different failure modes when it undergoes an impact either at low velocity or at high velocity. The damage modes are significantly different for low velocity impact and high velocity impact for the same specimen. Each layer has its own failure modes based on the damage it undergoes. The composite layer mostly retards the impactor by absorbing energy in tensile failure of primary fibers, deformation of secondary fibers and delamination. The dominant mode of energy absorption in PUF is crushing of the foam material. On the other hand, PUS absorbs impactor energy by deformation and shear plugging. SiC plate and inserts being hard and brittle largely absorbs energy in compression mode.
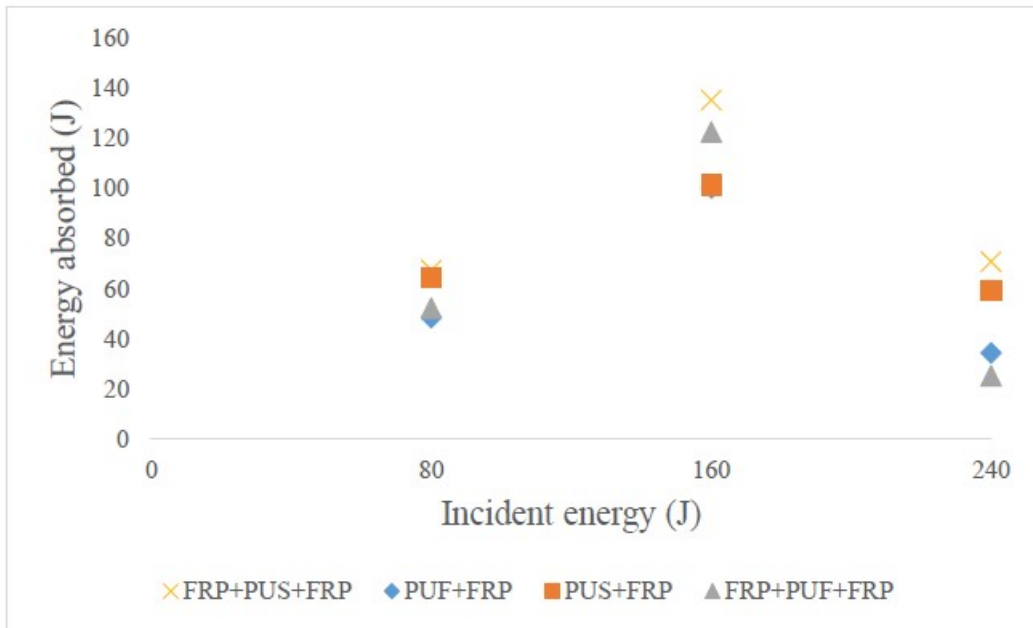
Fig. 6: *Energy absorbing trend of various target materials at different energy levels*

Figure 7 shows front, side and rear views of the PUS+GFRP specimen when it is subjected to 240J of incident impactor energy. Major delamination is observed in the surrounding region of the impacted area in the back end of the GFRP laminate. The delamination area in PUS+GFRP is 2400mm² which is greater than the delamination area in case of PUF+GFRP (1801 mm²), because of stiffness variation in the core material. PU Sheet is more elastically deformable than PUF. This excessive deformation of PUS caused more delamination in composite backing when compared to specimen having PUF.
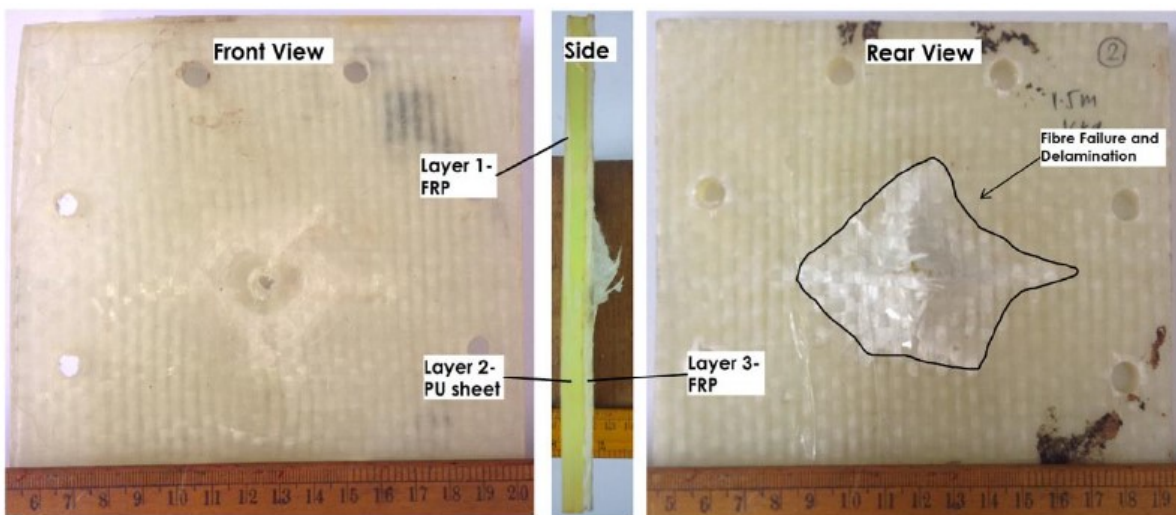

Figure 7: *PUS+GFRP laminate impacted at 240 J of incident energy*

The delamination area in PUS+GFRP specimen at 160J is about 1312 mm² and the delamination area in PUS+GFRP laminate at 80J is 1060 mm². For PUS+GFRP specimen, as the incident impactor energy is increased, the delamination at the back-end composite layer also increases significantly. Whereas, the GFRP+PUS+GFRP specimen has a decreasing trend of delamination as the incident energy is increased. The delamination area in the back-end GFRP laminate is 8103 mm² and 7900 mm² when GFRP+PUS+GFRP specimen is impacted at 80J and 160J respectively. At 240J of impact energy, the delamination area in GFRP+PUS+GFRP specimen is observed to be 1500 mm² (Balaganesan et al., 2017). Figure 8 consists of the front, side and rear view of GFRP+PUS+GFRP

laminate at 80J of impactor energy. This specimen absorbs maximum energy in delamination having 8103 mm² of delamination area as compared to other tested specimens at 80J, 160J and 240J. In this case, the impactor got stuck in the specimen and the energy transfer to the back end GFRP layer is by bending of PU sheet.
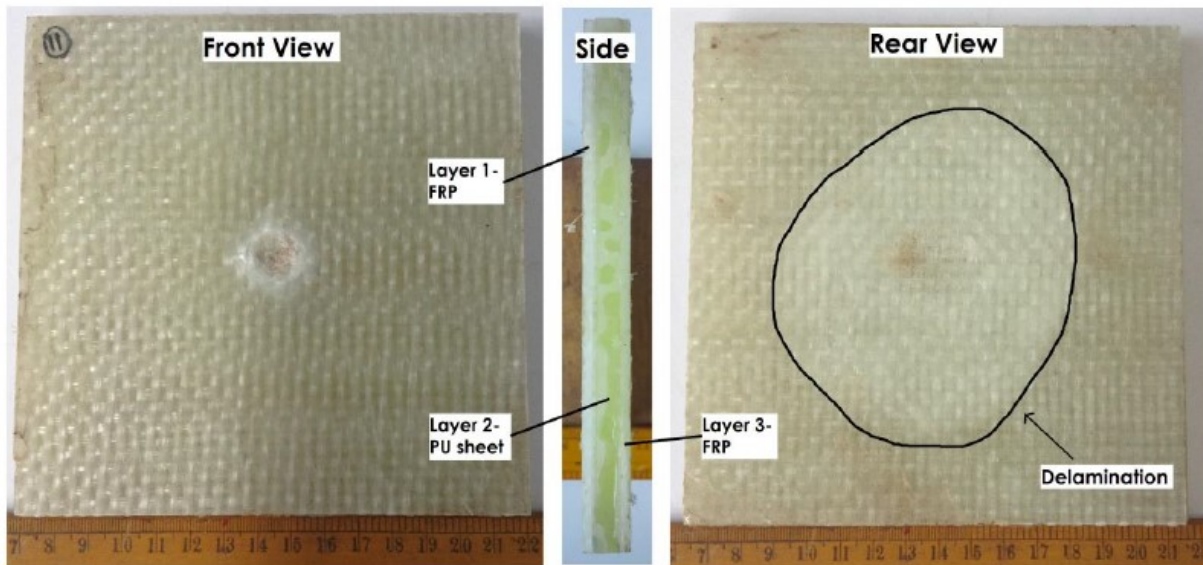

Figure 8: *Energy absorbed by GFRP+PUS+GFRP laminate impacted at 80j of incident energy*

But on reversing the laminate configuration. When the impact is done on the front GFRP layer, interesting observations are made. Figure 9 shows the front, side and rear view of this laminate. The front GFRP layer is penetrated, but the back-end PU sheet undergoes excessive bending and it is not penetrated.
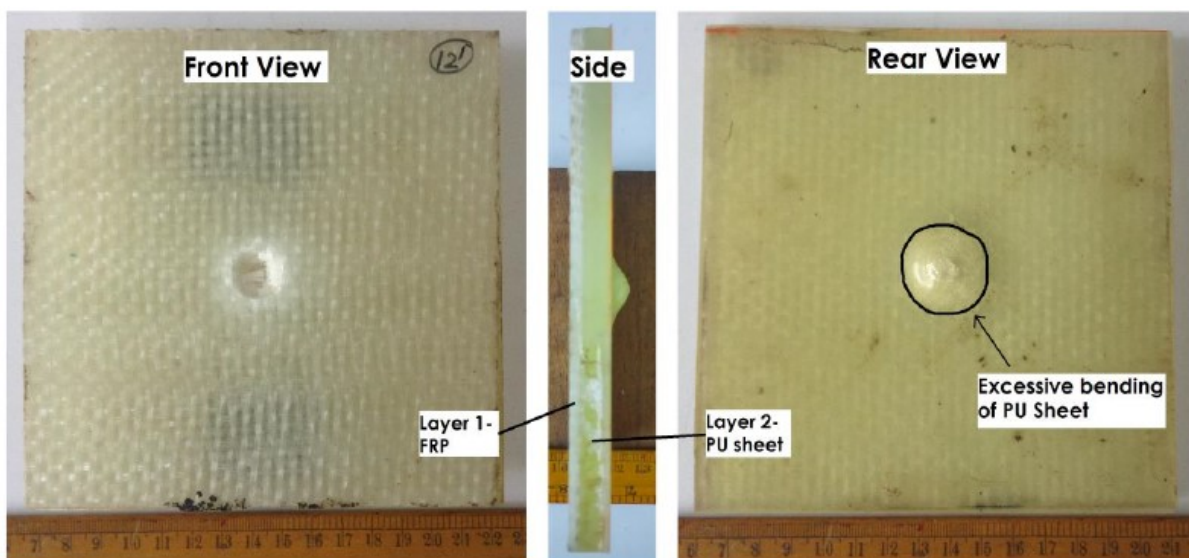

Figure 9: *GFRP+PUS laminate impacted at 80J of impactor energy*

Figure 10 shows the front, side and rear view of 6mm thick SiC plate layered over PUF+GFRP laminate which is subjected to impact at 160J of energy. When the projectile strikes the ceramic, a compressive stress wave is induced and that region of ceramic would be subjected to compressive stress, due to which the ceramic along the radial direction would be under tension. Therefore, radial cracks are formed which initiated at the point of impact and extended to boundary. The damage granules of SiC is seen in Figure 10. Delamination and failure of fibers is observed in the back end GFRP layer. The delamination area is observed to be 2120 mm². The fiber failure is ob-

served in the impacted area as well as in its surrounding area. The tensile failure of fibers in surrounding area is due to high stiffness and damage of SiC plate.

A sharp edge is formed on the ceramic due to the formation of radial cracks and compressive failure. This leads to the formation of scratches on the surface of the impactor due to chipping which is seen in Figure 11. When the impact velocity is less than the plastic wave velocity of the impactor, the deformation of the front end of the projectile take place. However, this deformation will stop if the relative velocity at the interface of the target material and the impactor reduces to zero (Naik et al., 2012).
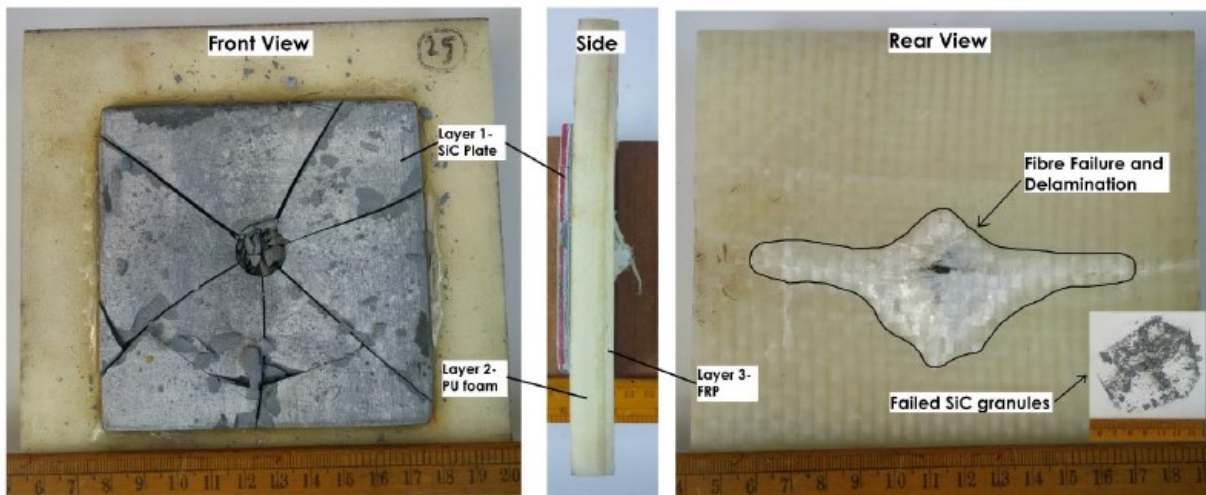

Figure 10: *Impact on 6mm thick front facing sic plate layered PUF/GFRP laminate at incident energy of 160J*
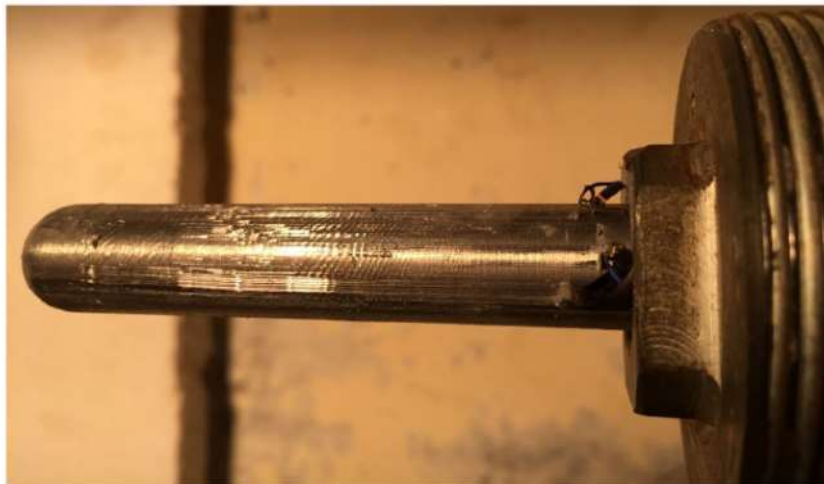

Figure 11: *Scratches and Chipping on the impactor due to sic layer*

The authors of this paper have explained the damage mechanisms and energy absorbed in each failure mode in their previous article (Balaganesan et al., 2017). Several experiments on various other combinations of materials are conducted to explain the phenomenon of high mass-low velocity drop weight impact experiments. They have developed an analytical model to quantize the energy absorbed in each failure mode. In the following sections, the authors have explained the numerical simulation of the specimen that are discussed in this paper as well as the specimen discussed in their previous article (Balaganesan et al., 2017). They have validated the numerical model for high mass-low velocity impact experiments to design the armor material for structural applications. The same numerical model is used to understand the ballistic performance of the armor i.e. the high velocity impact experiments.

5. NUMERICAL RESULTS

5.1 Low Velocity Impact

With the above finite element model presented, all experiments described in Section 2 are simulated to obtain energy absorbed by the laminate, contact force histories, total deformation, stress variation, deflection and damage area.

Figures 12 (a) to (d) show the results for the damage in the laminate made of PUS+GFRP sheet at various time steps ranging from start of the impact event till the end. It is observed that the impactor penetrates the specimen. The gradual increase in deflection of the laminate in Z direction and finally complete perforation failure as seen during the experiments can also be observed in figure 12. In numerical results, it is possible to obtain the deflection of moving cone from AUTODYN result files directly at different time steps during penetration. Also, maximum deflection is found out experimentally by analysing the high-speed movie clips.
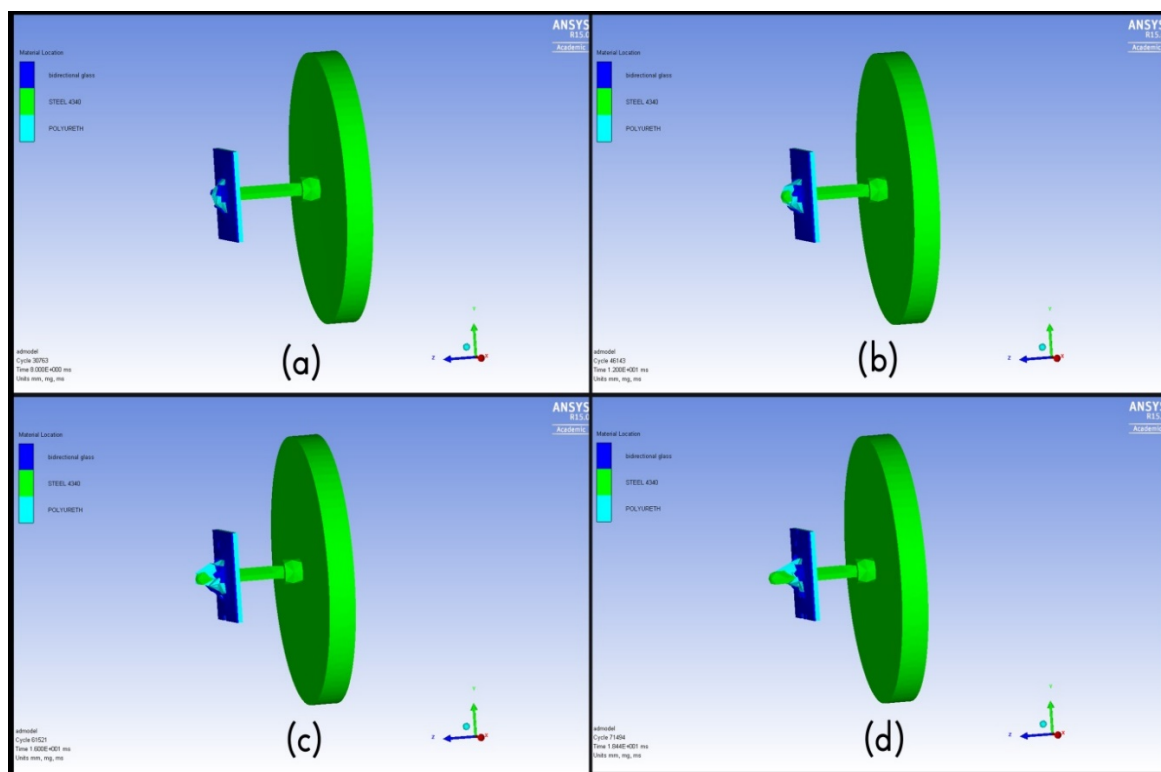

Figure 12: *Sequence of failure in PU sheet + composite laminate impacted at 80 J*

Table 2 shows for the numerical results for the energy absorbed by the sandwiched laminates for various energy of impactor. Figure 13 shows the kinetic energy and velocity of projectile during impact at 240 J for FRP+PUF+FRP specimen. The initial velocity of impactor at 5 m/s is given as input in the numerical analysis. It is observed that the perforation time is 2.82 m s. As expected both the parameters are decreasing with respect to time and it saturates once the impactor left the specimen. Similar trendis observed for other specimens also.

Table 2. Numerical results for the energy absorbed by the sandwiched laminates for various energy of impactor

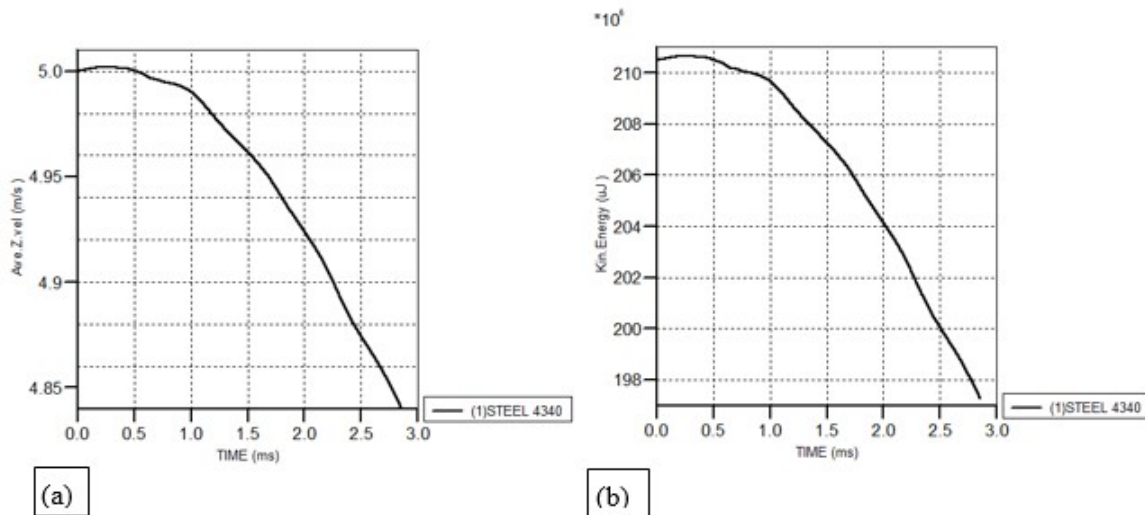| Specimen	Energy absorbed (J)		
	Impactor Energy (80J)	Impactor Energy (160J)	Impactor Enegy(240J)
GFRP	15.32		
PUF+GFRP	40.54	105.64	39.47
PUS+GFRP	70.83	107.59	50.89
FRP+PUF+GFRP	58.36	130.58	18.36
FRP+PUS+GFRP	72.62	146.87	77.65

.

Figure 13: *(a) velocity, (b) kinetic energy variation of projectile during perforation for FRP+PUF+FRP for impact at 1.5m*

5.2 High Velocity Impact

Upon establishing the low velocity impact experiments numerical model, the same model is extended and numerical simulation is carried out to understand the protective behaviour and energy absorbing capacity of the SiC bonded specimens in high velocity impact. As discussed earlier erosion of projectile is observed in case of impact onto SiC plates/inserts. Figure 14 shows the erosion of projectile for the SiC(10mm) + PUF + GFRP specimen impacted at 722 m/s. The residual velocity of projectile is 435 m/s and the specimen has absorbed 1328 J of energy. Table 3 shows the energy absorbed and residual velocity of SiC bonded specimens calculated numerically.

Table 3: energy absorbed by the sic layered target materials at high velocity impact in numerical simulation

Specimen	Initial velocity(m/s)	Residual velocity(m/s)	Energy absorbed (J)
SiC(10mm)+PUF(10mm)+GFRP	722	435	1328
SiC(6mm)+PUS(5mm)+GFRP	721	552	860
SiC(6mm Inserts)+PUF(10mm)+GFRP	732	581	793

Figure 15 shows the energy absorbed by 10mm thickness SiC layer of the specimen SiC(10mm) + PUF(10mm) + GFRP, when it is impacted at 722 m/s. It is understood that more than 40% of the total energy is absorbed by the SiC interface and then the eroded projectile further penetrates the foam and composite layer. Once the SiC layer is damaged then it cannot provide any more resistance to impact.
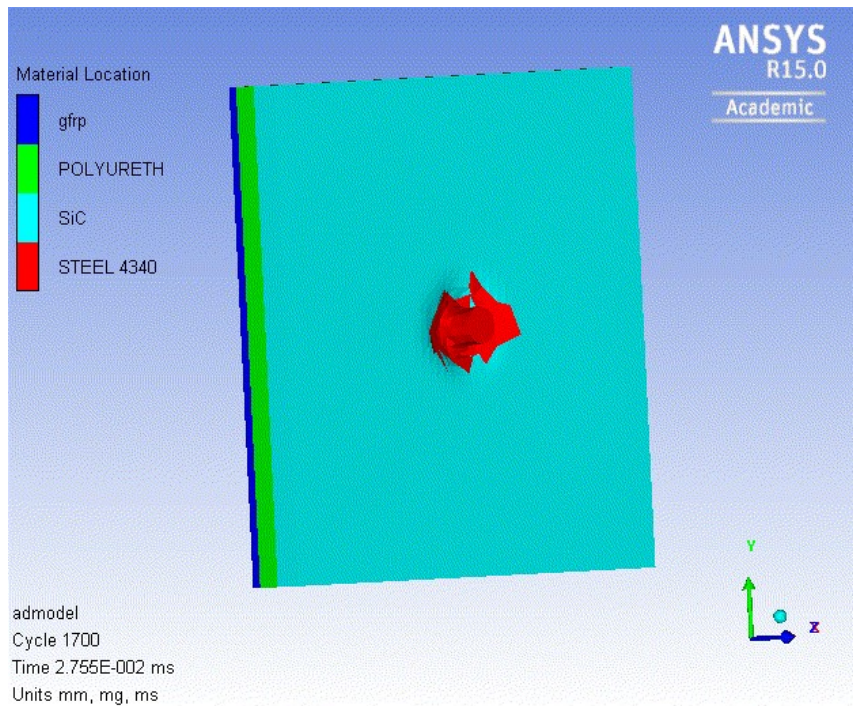
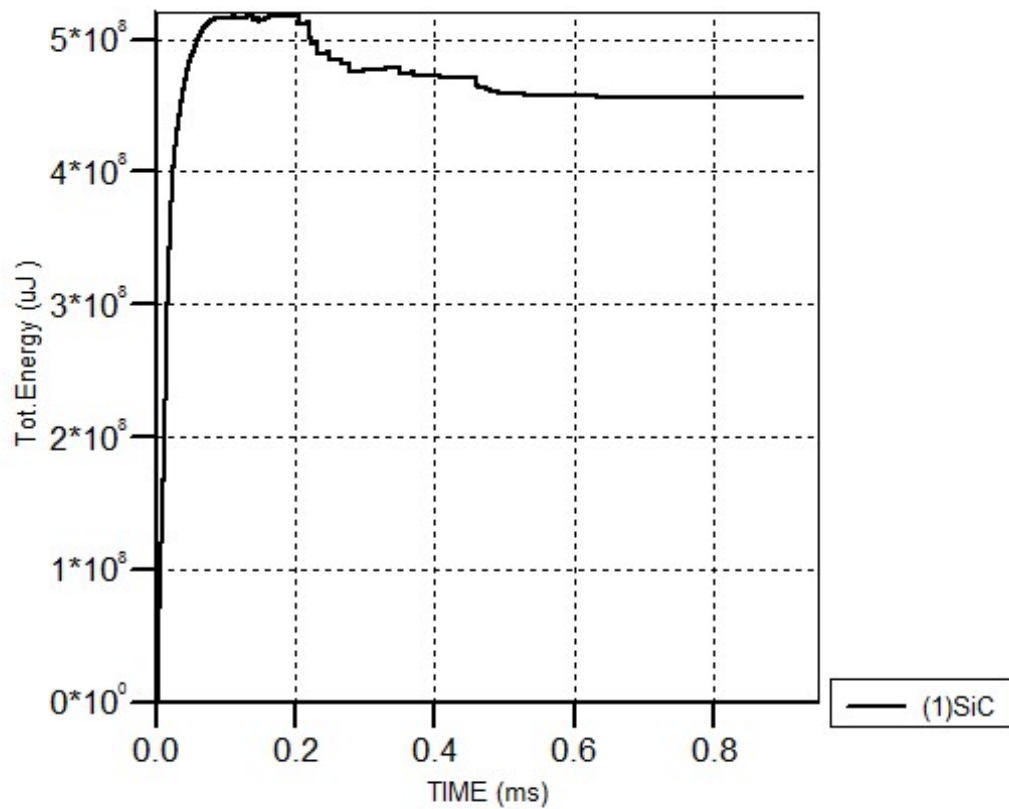**Figure 14:** *SiC (10mm) +PUF+ GFRP specimen subjected to impact at 722 m/s*

Figure 15: *Total energy absorbed by only sic layer during impact of SiC (10mm) + PUF+FRP specimen at 722 J*

6. COMPARISON OF NUMERICAL AND EXPERIMENTAL RESULTS

6.1 Energy absorption in various laminates at different energy level

Numerical simulation and experiments are carried out for different incident energy levels. The energy absorbed by the laminates for impact loading at 0.5m height (80 J) is shown for both experimental and numerical values in Figure 16. A good agreement is found between the two. Both experimental and numerical studies revealed that energy absorbed by specimen GFRP+PUS+GFRP is better when compared with the other sandwiched specimens. Both studies show that PUS+GFRP and GFRP+PUS+GFRP have absorbed same level of energy. The additional composite layer has not contributed significantly towards the structural performance.
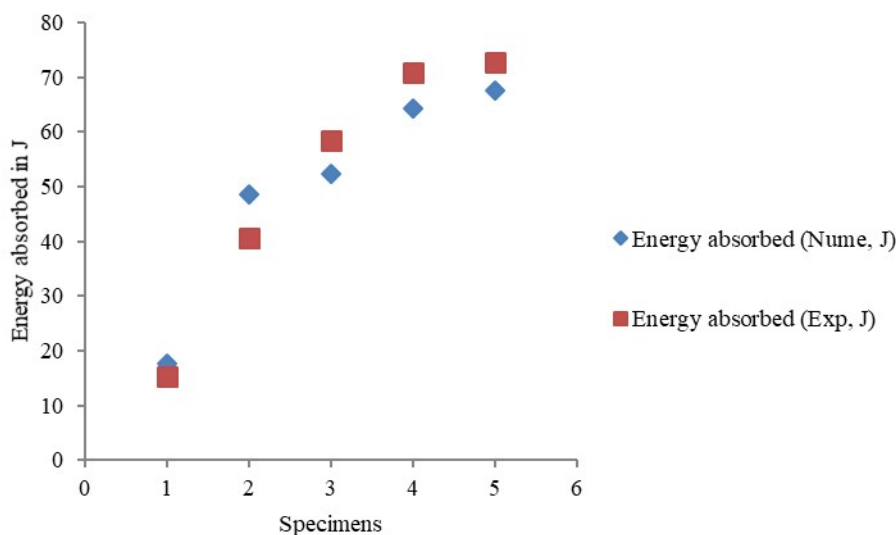

Figure 16: Comparison of energy absorbed numerically and experimentally at when the incident energy was 80 J

The maximum deflection in z-direction for PUS+GFRP specimen is obtained by both numerically as well as experimentally at different impactor energy and are compared in Table 4. It is seen that maximum deflection value before failure increases as the energy level increases, but it is observed up to 160 J impactor energy, at 240J, the specimen is penetrated and the deflection is significantly reduced. Once it is penetrated completely, it cannot provide any resistance to impact and hence deflection reduces.

Table 4: Comparison of deflection value for PUS+FRP specimen

Impactor Energy, J	Deflection (Numerical, J)	Deflection (Experiment, J)
80	19.896	15.8775
160	36.89	40.54
240	24.563	19.442

The damage pattern of the laminate of PUS+GFRP impacted at 160 J is shown in Figure 17 (a). The cross section of fiber failure and debonding between the PUS+GFRP layer are shown in Figure 17 (b). The composite backend delamination is also observed. Figures 18 (a), (b) and (c) show for the target material that is subjected to impact during experiment. A comparison is made between numerical and experimental damage and the results are reasonably matching. It is observed that the outer PUS layer is damaged and coming out in both cases accompanied by fiber failure. In test a bulge in the PUS in the rebound direction of impactor is also observed.
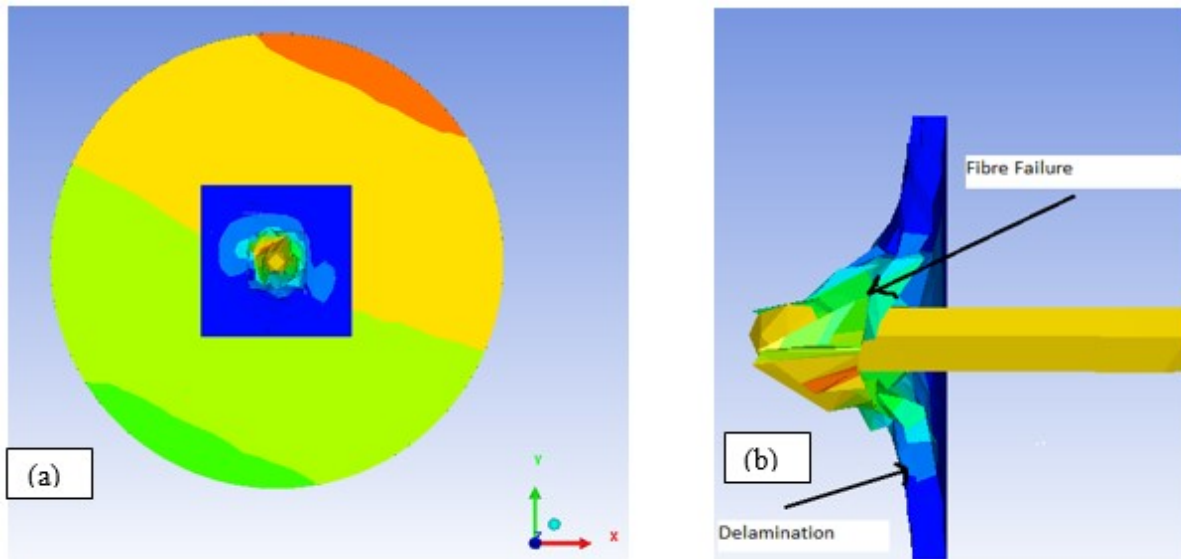
Figure 17: *(a) Numerical result image for laminate subjected to impact at 160 J (b) cut section view of numerical simulation of the laminate*
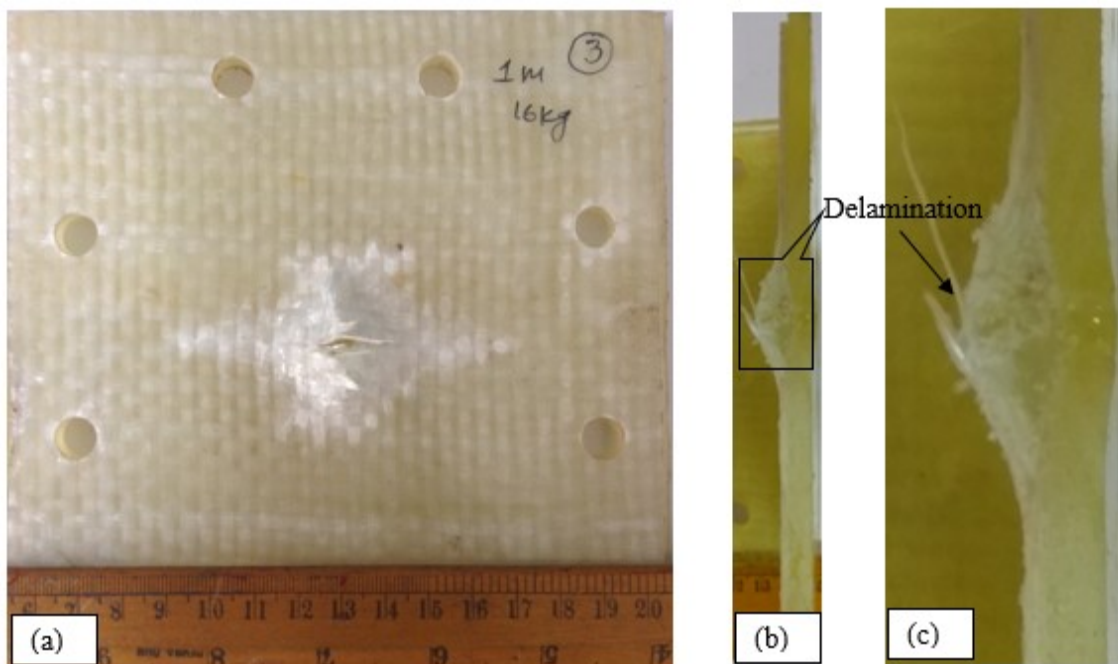

Figure 18: *(a) Test image for laminate subjected to impact at 160 J (b) cut section view of the laminate observed after test (c) zoom in view of cut section*

Figure 19 show the energy absorbed values of ceramic laminates subjected to 240J impact energy by experimental and numerical techniques. A good agreement is seen. It is observed in numerical simulation that the damage in case of SiC inserts are only local whereas in case SiC plates, the entire specimen is failed. Moreover, the composite back face damage is also very minimal in case of inserts than plates. The energy absorbing capacity of PUF+GFRP specimen increases by three times when SiCmaterial is bonded as front facing material. The specimen containing 10 mm thick SiC plate layered over PUF+GFRP absorbed 12% more energy than the specimen containing 6 mm SiC plate layered over PUF+GFRP. The energy absorption of 6 mm thickness SiC inserts layered PUF/GFRP laminate is 16% less when compared to 6 mm thickness SiC plate layered PUF/GFRP laminate. It is also observed that the damage in case of inserts is constrained to area under the impact unlike plate.
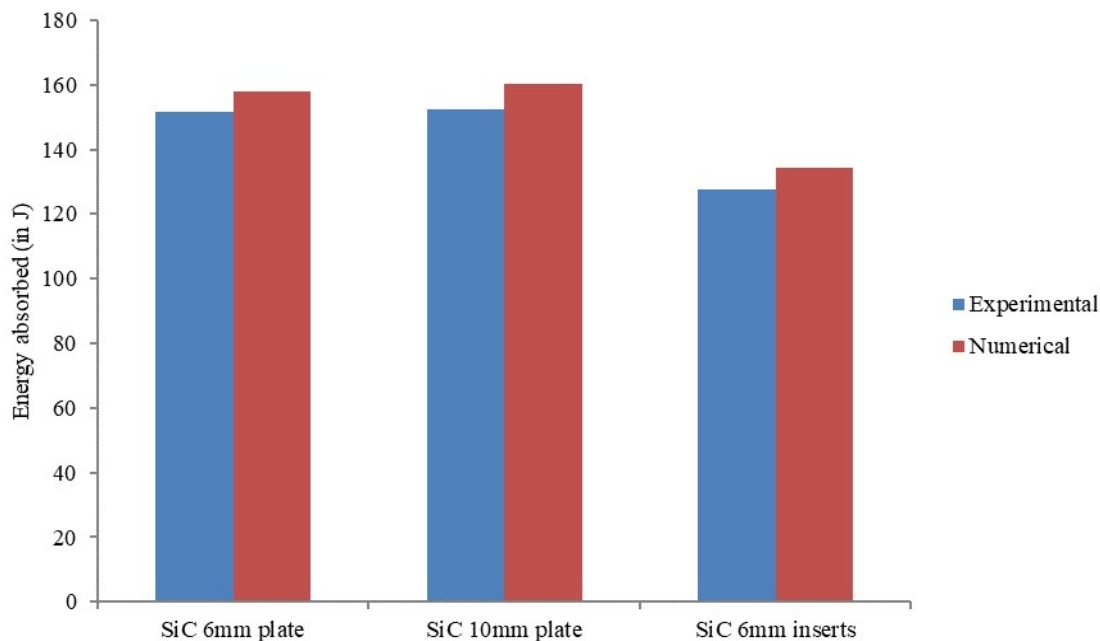
Figure 19: *Comparison of energy absorbed numerically and experimentally at 240 J*

7. CONCLUSIONS

An experimental study is carried out for multilayer target material having various combinations of PUF, PUS and SiC plate/inserts with back end material as GFRP to understand their energy absorbing capacity during impact loading. Numerical simulation is carried out to validate the experimental results. The following conclusions are made based on the study:

• At 80 J of impactor energy, the specimen GFRP+PUF is penetrated whereas GFRP+PUS is not penetrated and the impactor is rebounded with 16 J of energy which shows the better performance of PUS as compared to PUF towards impact.
• Extent of delamination in the backend GFRP is very high when it is bonded with PUS than PUF.
• Introduction of SiC plates/inserts as front layer increases the impact resistance as well structural performance.
• The 10mm thickness SiC plate layered target absorbs 12% more energy than 6mm thickness SiC plate layered target material.
• The ballistic performance of SiC(6mm plate)+PUS+GFRP and SiC(6mm Inserts)+PUF+FRP are same at high velocity impact, but damage is local in case of SiC inserts layered target and it can also undergo multiple impacts at different locations.
• Good agreement is seen between the results of numerical modelling and experimental.

References

Abdel-Nasser Yehia, Elhewy Ahmed M.H. and Al-Mallah, Islam (2016). Impact analysis of composite laminate using finite element method, Ships and Offshore Structures,12(2): 219-226. DOI: 10.1080/17445302.2015.1131005

Akshaj K. V., Surya P., Pandit, M.K. (2017). Low Velocity Impact Response of Composite/Sandwich Structures, Key Engineering Materials, 725, 127-131.

Balaganesan G and Chandra Khan V, (2016). Energy absorption of repaired composite laminates subjected to impact loading, Composites Part B, 98: 39-48. doi: 10.1016/ j.compositesb.2016.04.083.

Balaganesan G, Velmurugan R, Srinivasan M, Gupta N. K., and Kanny K. (2014). Energy absorption and ballistic limit of nanocomposite laminates subjected to impact loading, International Journal of Impact Engineering, 74:57-66.

Balaganesan, G. V., Akshaj Kumar, V. C., Khan and Srinivasan, S. M. (2017). Energy Absorbing Capacity of Polyurethane/SiC/Glass-Epoxy Laminates under Impact Loading, Journal of Engineering Materials and Technology, 139(2):021008.

Bhatnagar A, (2006). Lightweight ballistic composites: military and law-enforcement applications, CRC Press.

Century Dynamics. 2013. ANSYS Autodyn User's Manual, Release 15.0.

Feli S. and Asgari M.R. (2011). Finite element simulation of ceramic/composite armor under ballistic impact, Composites: Part B, 42:771–780

Ferreño Diego, Carrascal Isidro A., Cicero Sergio and Meng, E. (2010). Characterization of Mechanical Properties of a Shock Absorber Polyurethane Foam for Elevators. Numerical Fitting of Mechanical Behavior Models for Hyperelastic and Elastomeric Foam Materials, Journal of Testing and Evaluation, 38 (2): 211-221.

Ghalami-Choobar Mehran and Sadighi, Mojtaba (2014). Investigation of high velocity impact of cylindrical projectile on sandwich panels with fiber–metal laminates skins and polyurethane core, Aerospace Science and Technology, 32:142–152

Ghosh A. and Sinha P.K. (2005). Initiation and propagation of damage in laminated composite shells due to low velocity impact, International Journal of Crashworthiness, 10:4, 379-388, DOI: 10.1533/ijcr.2005.0354

Holmquist TJ and Johnson GR. (2002). Response of silicon carbide to high velocity impact, J ApplPhys, 91(9):5858–66.

Inai R, Chirwa E C, Saito H, Uozumi T, Nakai A and Hamada, H (2003). Experimental investigation on the crushing properties of carbon fibre braided composite tubes, International Journal of Crashworthiness, 8:5, 513-521, DOI: 10.1533/ijcr.2003.0253

Johnson GR and Holmquist TJ. (1994). An improved computational constitutive model for brittle materials, In: High pressure Science and technology, New York: American Institute of Physics, 981-984.

Johnson GR and Holmquist, TJ. (1990). A computational constitutive model for brittle materials subjected to large strains, high strain rates, and high pressure, Proceedings of EXPLOMET conference, San Diego.

Karandikar P. G. (2009). A review of ceramics for armor applications. The American Ceramic Society, Advances in Ceramic Armor IV, 29:163–175.

Kauffmann C, Cronin D, Worswick M, Pageau G and Beth A. (2003). Influence of material properties on the ballistic performance of ceramics for personal body armor. Shock Vib, 10:51–58

Krishnan K, Sockalingam S, Bansal S and Rajan SD. (2010). Numerical simulation of ceramic composite armor subjected to ballistic impact, Compos Part B Eng., 41:583-93.

Long Shuchang, Yao Xiaohu and Zhang Xiaoqing (2015). Delamination prediction in composite laminates under low velocity impact, Composite Structures, 132:290–298.

Morye S.S, Hine P.J, Duckett R. A., Carr D.J, Ward I.M, (2000). Modeling of the energy absorption by polymer composites upon ballistic impact, Composites Science and Technology, 60:2631-2642.

Naik, N. K., Kumar, S., Ratnaveer, D., Joshi, M., and Akella, K. (2012). "An Energy-Based Model for Ballistic Impact Analysis of Ceramic-Composite Armors," Int. J. Damage Mech., 22(2):1–43.

Ogden, R. W. (1972). Large deformation isotropic elasticity – on the correlation of theory and experiment for incompressible rubberlike solids, Proc. R. Soc. Lond., A, 326:565–584.

Qiao P, Yang Mijia and Bobaru Florin, (2008). Impact Mechanics and High-Energy Absorbing Materials: Review, Journal of Aerospace Engineering 21:4, 235–248

Quan, X, Clegg RA, Cowler MS, Birnbaum NK and Hayhurst CJ. (2006). Numerical simulation of long rods impacting silicon carbide targets using JH-1 model, International Journal of Impact Engineering, 33:634–644

Sekine H., Hu N., Fukunaga H. and Natsume T. (1998). Low velocity impact response of composite laminates with a delamination, Mechanics of Composite Materials and Structures, 5:3, 257-278.

Shim V.P.W., Tu Z.H. and Lim C.T. (2000), Two-dimensional response of crushable polyurethane foam to low velocity impact, International Journal of Impact Engineering, 24:703-731.

Velmurugan R, Ganesh Babu M and Gupta N K (2006). Projectile impact on sandwich panels, International Journal of Crashworthiness, 11:2, 153-164, DOI: 10.1533/ijcr.2005.0385. Online link: http://dx.doi.org/10.1533/ijcr.2005.0385

Velmurugan R. and Balaganesan G. (2013). Energy absorption characteristics of glass/epoxy nano composite laminates by impact loading, International Journal of Crashworthiness, 18:1, 82-92.

Wang Jie, Waas Anthony M. and Wang Hai (2013). Experimental and numerical study on the low-velocity impact behavior of foam-core sandwich panels, Composite Structures, 96:298–311.

Wilkins ML, (1978). Mechanics of penetration and perforation, Int J EngSci, 16:793-807.

Yazdani Nezhad, H., Merwick, F., Frizzell R.M. and McCarthy C.T. (2015). Numerical analysis of low-velocity rigid-body impact response of composite panels, International Journal of Crashworthiness, 20:1, 27-43, DOI: 10.1080/13588265.2014.963378

Zhang Guoqi, Wang Bing, Ma Li, Wu Linzhi, Pan Shidong and Yang Jinshui (2014). Energy absorption and low velocity impact response of polyurethane foam filled pyramidal lattice core sandwich panels, Composite Structures, 108:304–310.